

What can transit timing variations tell us about orbital decay and stellar structure?

Lawrence Berry

March 2024

Abstract

In this essay, I will present an overview of exoplanet detection methods and discuss how the transit method can be used to study the orbital evolution of giant close-in exoplanets known as hot Jupiters. My project is motivated by a desire to better understand the structure of stars, including the mass and depth of their convective envelopes, and I will discuss how modelling one class of evolutionary effects - tidal interactions - could serve as a possible new tool with which to investigate stellar structure. Finally, I conclude by outlining the open problems in this field and discuss my project's stated goal and methodology.

1 Introduction

1.1 Background

The first planets outside our solar system were identified around a radio-pulsar neutron star by Wolszczan and Frail in 1992 by analysing changes in the apparent pulsation period of the star caused by a Doppler shift due to the pulsar's orbit around the barycentre of the star-planet system [35]. Three years later, Queloz and Mayor became the first to discover such a planet orbiting a main-sequence star, a feat for which they were awarded the Nobel Prize in 2019. Since main-sequence stars do not pulse brightly they employed a different but analogous method: observing periodic variations in the star's radial velocity using the Doppler shift of its spectrum [23].

Since then more than 5000 so-called exoplanets have been discovered. Some have been identified using the same radial velocity technique employed by Queloz and Mayor, but the majority have been identified by looking at changes in the brightness of a star as exoplanets transit its disc. Two space-based telescopes exploiting this technique, Kepler and TESS, together contributed an impressive 3000 of these confirmed planets [26].

Just 30 years ago we knew of only 8 planets within our solar system. Today we have observational data from thousands of planets orbiting thousands of stars. The ages of these planets vary wildly, allowing us to glimpse stellar systems at various stages of planetary formation and help us understand how stellar systems (including our own) evolve over time. In addition, the ever-growing sample size has made it possible to study planets in a statistical manner and make broader inferences about the processes that

affect the formation and evolution of planetary systems, such as through occurrence rate studies of different types of planets. In this project however, I will perform a statistical analysis not of planetary characteristics, but of planetary orbits and, more specifically, their evolution over time.

1.2 Orbital evolution

As we enter the fourth decade of exoplanet discovery, a field of growing interest is the study of orbital evolution: how planetary orbits change over time. The physical processes which affect orbits are typically slow acting (on the order of ms/year for the most extreme decay mechanisms). Combined with the limited precision of experimental equipment, it can take decades of observations to conclusively model even the most extreme changes in planetary orbits. Since the observation of exoplanets began in the 1990s and took off more widely with the launch of dedicated telescopes like WASP in 2006 and Kepler in 2009, only recently have we acquired enough data to make such analysis possible.

A typical Keplerian orbit may change over time, or appear to change over time as viewed from Earth, due to a number of different physical or apparent phenomena: [29]

1. **Actual** physical effects: these are caused by the presence of a non-Keplerian gravitational potential. That is to say, a potential which is not simply inversely proportional to radius or is not spherically symmetric. This could be caused by:
 - (a) Rotational oblateness of star or planet. As a star or planet spins centrifugal forces cause it to bulge at the centre, perpendicular to its axis of rotation. Such a bulge creates a gravitational force inversely proportional to the cube of radial distance, an effect known as a quadrupole moment.
 - (b) The presence of perturbing companion planets or moons.
 - (c) General relativistic effects, which can cause a precession of the orbit in addition to what might be expected under Newtonian physics. In fact, explaining the above-expected precession of Mercury was one of the first major successes of GR.
 - (d) Tidal interactions: tidal influences which add or take away energy from the planet (primarily those raised by the planet on the star but potentially also star on planet or planet on planet).
2. There are also **apparent** effects in which orbits appear to change due to the relative motions of the Earth and the stellar system being observed (though in reality they do not). These include:
 - (a) Changes in geometrical projection due to parallax or proper motion of the star. For example, if a star shifts position in the sky over time, transits observed from Earth will be seen from a slightly different angle.
 - (b) Line of sight accelerations: orbital periods may appear to get larger when the star-planet system accelerates away from the Earth. For example, this could be caused by the gravitational influence of a large wide-orbiting planet, which Bouma et al invoke to explain transit timing variations in Wasp-4b [4].

After accounting for apparent effects described in point 2, orbital evolution provides a means to investigate the various physical effects described in point 1. In particular, this essay is going to focus on the evolutionary effects caused by tidal interactions, and how it relates to stellar structure.

1.3 Motivation

The study of orbital evolution could help answer a variety of interesting research questions.

1. How is it possible that large planets can be found so close to their host star despite the relative lack of material in the proto-planetary disk at such distances? Have these planets formed further out and migrated inwards over time, or were they formed as the result of planetary collisions? Perhaps the observed paucity of rocky inner planets in systems containing a hot Jupiter [12] may provide evidence for migration theories, as migrating hot Jupiters could have disturbed the orbits of any inner planets that used to be in the system.
2. Are there other planets that we can't see? Observations of orbital evolution could help infer the presence of other planets or moons in a system when such bodies can't be detected by other means: perhaps because the body is too small to produce a detectable transit or radial-velocity signal, or because its orbital inclination relative to our line of sight is too large for these methods to work well.
3. What are the interiors of stars and planets made of? The strength of tidal interactions between stars and planets is a direct consequence of stellar and planetary composition and structure. Such tidal interactions cause changes in orbits over time (usually evident as a decay in semi-major axis), and as a result could tell us something about the star and planet's interior.

This project will focus primarily on the third of these research questions, the study of tidal interactions and what it can tell us about stellar and planetary structure. It is a particularly important question given few other tools exist today for studying stellar and planetary interiors.

In the context of stellar structure there is asteroseismology (studying the oscillations in stellar brightness over time), or stellar spectroscopy (studying the wavelength dependence of stellar light). For planetary structure our options are even more limited. To date, observational research of planetary structure has been limited to the study of close-in transiting exoplanets like WASP-103b, a giant planet whose tidal deformation is so extreme it is apparent in transit light-curves [2]. Such extreme deformation is rare, but tidal interactions of a significant magnitude are theoretically expected to be more common. High-precision spectroscopic instruments on large telescopes like the VLT and James Webb can be used to study atmospheres by measuring the spectrum of stellar light absorbed by a planet's atmosphere during a transit, but it can't be used to glean what's under the surface.

The main goal of this project will be to identify instances of exoplanetary orbital evolution caused by tidal interactions and fit models to these interactions. Finally, the

models will be used to infer stellar characteristics. To do this we will make use of publicly available transit data for large close-in Hot Jupiter exoplanets from a variety of professional telescopes and citizen-scientist sources. Deviations in these transit times from what might be expected under the assumption of no orbital evolution, known as “transit timing variations” will be computed and used to identify orbital decay. Modelling the decay of these planets will be useful for testing the theory of tidal interactions, as well as investigating stellar structure - specifically, the distribution of material within stars and the mass and depth of convective envelopes. Some of the techniques developed in the process may be useful in understanding other orbital evolution phenomena too.

2 Comprehensive literature review

2.1 How can exoplanets be detected?

There are five primary methods of exoplanet detection. These are summarised as follows:

1. **Radial velocity**, the original method used by Queloz and Mayor [23]. This technique involves analysing the Doppler shift in the spectrum of light received from a star to infer its radial velocity towards or away from us. This radial velocity will subtly change if the star is orbiting a barycentre that does not coincide with its own centre. This can happen if there is a significantly massive enough planet orbiting the star, in which case the planet and star move around a common centre of gravity that is slightly offset from the star’s centre. The star’s radial velocity will appear to oscillate as it orbits this common centre of gravity.

The method can provide information on the period and eccentricity of the planet but can only provide a lower bound on its mass due to a degeneracy with inclination. Example instruments applying this method include the ground-based HARPS spectrographs.

This technique favours the detection of shorter period, massive planets orbiting lower mass stars whose orbital plane lies close to our line of sight. These systems will have a barycentre furthest from the centre of the star and so the star will exhibit a greater change in radial velocity.

2. **Transits**, the method responsible for the most exoplanet detections to date. It involves imaging the star at a regular cadence to capture a reduction in brightness as orbiting planets pass in front of the star. This is analogous to other transits that happen in our own solar system, such as the transits of Mercury and Venus. However observing transits at such a distance requires a good deal higher precision as the flux intensity is orders of magnitude smaller. With the most sensitive equipment occultations of a planet as it passes behind the star can also be distinguished, which can be useful for distinguishing between the effects of decay and precession.

The shapes of several successive light curves can be used to model the orbital parameters of a system, as well as planetary mass and radius if the mass and radius of the host star are known. During transits, light from the star passes through the atmosphere of the planet. As a result, suitably high-resolution spectrographs can be used to analyse absorption lines and infer atmospheric composition.

Example instruments using this method include the Kepler and TESS space telescopes. This technique favours the detection of large planets whose orbital plane lies directly in our line of sight and are close to their star (the probability of a transit being observable is smaller the further away it is, and the planet’s orbital period makes it improbable that it will be observed in a given limited observing window),

Three additional but less widely used techniques:

3. **Astrometry**, which uses high-precision measurements of the angular position of stars in the sky to observe the motion of stars about their barycentres. This is analogous to the radial velocity technique, but measuring oscillations of the star perpendicular to our line of sight.
4. **Direct imaging**, which involves imaging a star using a coronagraph or sunshade to suppress light from the star, allowing direct observations of any planets orbiting it, so long as the orbital radius is greater than the imager’s angular resolution.
5. **Gravitational microlensing**, which involves monitoring for lensing events that occur when a stellar system containing a planet passes in front of a background star. The background star appears to increase in brightness as its light is focused by the foreground system due to general relativistic effects. These events are unpredictable and difficult to systematically observe.

Of particular interest in the context of this project are a class of exoplanets known as “Hot Jupiters”. These are gas giant exoplanets with an orbital period of typically less than ten days. They orbit in close proximity to their host star and earn their name due to high surface atmosphere temperatures. As a result of their large mass and close proximity, they are expected to experience particularly large tidal interactions. Consequently, much of the work in this field makes use of transit observations because the transit method has a strong bias towards detecting large planets at short orbital periods as discussed.

In addition transits are relatively cheap to observe: they do not require expensive spectroscopic equipment, merely a reasonably sensitive CCD and a clear night sky. Therefore transit data is plentiful compared to radial velocity observations which require expensive spectrometers, or direct images or astrometric measurements which require extreme precision beyond the capabilities of all but the most cutting edge experiments. Microlensing meanwhile can’t be used to study orbital evolution because lensing events are one-offs that do not regularly recur.

There are several databases dedicated to collecting transit observations made by citizen-scientists using hobby telescopes, such as the Czech Astronomical Society’s Exoplanet Transit Database, which Hagey et al used in their 2022 study of transit timing variations in 30 systems [10]. A similar project run out of UCL, ExoClock, is collating transit observations for the purpose of developing an observing schedule for the upcoming ARIEL mission [20]. Transit observations will therefore be the main source of data for this project.

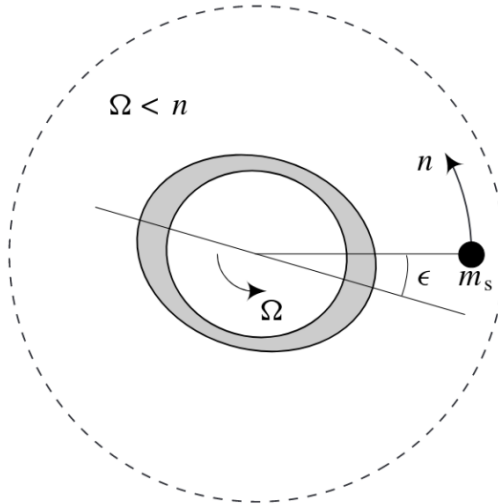


Figure 1: The tidal bulge raised on a star by an orbiting planet lags by some characteristic angle ϵ [24].

2.2 What is tidal decay?

The study of tidal interactions dates back to the early 1700s when Edmond Halley used the then brand new theory of Newtonian mechanics to model the timings of solar eclipses. Despite predicting the 1715 total solar eclipse over the UK with groundbreaking precision, he soon encountered a problem: his predicted eclipse timings differed slightly from historical accounts. He correctly identified that either the Moon must be speeding up, or the Earth slowing down [25].

In 1749 Richard Dunthorne linked the two and proposed that angular momentum was actually being transferred from the Earth to the Moon, causing the Earth's rotation to slow down whilst the Moon sped up. In 1754, Immanuel Kant discussed the decelerating effect of the ocean tides on the Earth's rotation and in 1848 Mayer identified this as the mechanism behind the transfer of angular momentum: the tides induced by the Moon on the Earth are causing the Earth's rotation to slow down and the Moon to speed up [18].

The first full quantitative theory was posited by George Darwin in a series of papers in 1879 and 1880 [5]. Similar mechanics apply to other bodies in the solar system, as explored by Goldreich in 1963 [7]. A particularly famous example is that of the Jovian moon Io, which experiences extreme volcanic activity on its surface due to the immense tidal forces exerted by Jupiter.

Exoplanets too undergo similar tidal interactions. Stellar tidal decay occurs when an orbiting planet exerts a gravitational force on its host star. This creates a tidal bulge which distorts the shape of the star, making it more oblate and creating a non-Keplerian gravitational potential. If the angle formed by the planet's orbit around the star leads the angle of the tidal bulge, then a potential gradient arises that causes the planet to experience a decelerating torque which slows it down, and conversely by conservation of angular momentum, speeds up the rotation of the star (see Figure 1).

What follows is a quantitative assessment of this effect based on the work of Murray and Dermott's *Solar System Dynamics* (2000), Goldreich and Soter (1966) and Greenberg

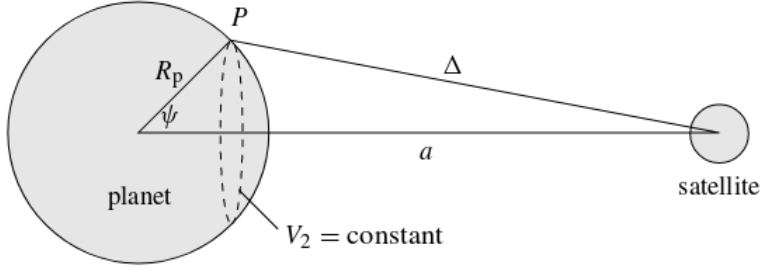


Figure 2: Geometry of a planet-satellite system presented by Murray (2000), also applicable to a star-planet system [24].

(2009), modified for conciseness and clarity:

1. Consider the gravitational potential ϕ of the planet evaluated at a point P on the surface of the star (see Figure 2):

$$\phi = -\frac{GM_*}{\Delta}$$

By the cosine rule:

$$\Delta = a \left(1 - 2 \left(\frac{R_*}{a} \right) \cos \psi + \left(\frac{R_*}{a} \right)^2 \right)^{\frac{1}{2}}$$

Given $R_* \ll a$, we can expand out binomially:

$$\begin{aligned} \Delta^{-1} &\approx a^{-1} \left(1 + \left(\frac{R_*}{a} \right) \cos \psi + \frac{3}{2} \left(\frac{R_*}{a} \right)^2 \cos^2 \psi - \frac{1}{2} \left(\frac{R_*}{a} \right)^2 + \frac{3}{8} \left(\frac{R_*}{a} \right)^4 \right) \\ &\approx a^{-1} \left(1 + \left(\frac{R_x}{a} \right) \cos \psi + \frac{1}{2} \left(\frac{R_*}{a} \right)^2 (3 \cos^2 \psi - 1) \right) \\ \phi &\approx -\frac{GM_*}{a} \left(1 + \left(\frac{R_*}{a} \right) \cos \psi + \frac{1}{2} \left(\frac{R_*}{a} \right)^2 (3 \cos^2 \psi - 1) \right) \\ &= \phi_1 + \phi_2 + \phi_3 \end{aligned}$$

Since $\frac{F}{M_p} = -\nabla \phi$, the first potential does not correspond to a force since it is constant. The second potential corresponds to a uniform acceleration that causes the body's standard Keplerian orbit about the system's barycentre. It is the higher order terms which produce the tidal bulge, approximated as:

$$\begin{aligned}
\phi_3 &= -\frac{1}{2} \frac{GM_p}{a} \left(\frac{R_*}{a} \right)^2 (3 \cos^2 \psi - 1) \\
&= -\frac{GM_p}{a^3} R_*^2 P_2(\cos \psi) \\
&= g \zeta P_2(\cos \psi)
\end{aligned} \tag{1}$$

Where:

- $\zeta = \frac{M_p}{M_*} \left(\frac{R_*}{a} \right)^3 R_*$, the amplitude of the tidal equipotential. This is a measure of the ratio of the tidal gravitational field strength due to the planet $\frac{GM_p R_*}{a^3}$ over the gravitational field strength of the star $g = \frac{GM_*}{R_*^2}$.
 - $g = \frac{GM_*}{R_*^2}$, the gravitational field strength of the star at its surface.
 - P_2 is known as the Legendre polynomial of degree 2 in $\cos \psi$. Note that $P_2(\cos \psi)$ has maximums at 0 and π , causing two tidal bulges per orbital period. This explains why the Earth experiences two high tides every day. The tidal bulge results from the potential gradient $F = -\nabla \phi_3$ across the width of the star.
2. The shape of the tidal bulge created by this tidal potential depends on the elastic forces within the star. Less rigid materials are more easily stretched by the tidal force, creating the ocean tides we see on Earth. The deformation of a homogeneous body can be described by:

$$R(\psi) = R_* (1 + h \zeta P_2(\cos \psi)) \tag{2}$$

Where h is one of the so-called Love numbers defined as the ratio of the body's deformation to the height of the tidal equipotential. A completely rigid body would have $h = 0$ such that its surface does not deform in any way. For a perfectly elastic fluid which flows perfectly towards the tidal equipotential (like the oceans on Earth), $h = 1$.

3. The external potential due to this bulge, using a similar calculation as above, is given by:

$$\phi_{\text{ext}} = -k \zeta g \left(\frac{R_*}{a} \right)^3 P_2(\cos \psi) \tag{3}$$

Where $k = \frac{3}{5}h$, another so-called Love number defined as the ratio of the additional potential created by the deformation over the original deforming potential.

4. This external potential induces a torque on the planet due to the fact that it is not axisymmetric (due to dependence on angle ψ):

$$\begin{aligned}
T &= M_p a \times -\frac{\partial \phi_{\text{ext}}}{\partial \theta} \\
&= -\frac{3}{2} \frac{GM_p}{a} \left(\frac{R}{a} \right)^5 k \sin 2\epsilon
\end{aligned}$$

Using the fact that $\frac{\partial P_2(\cos \psi)}{\partial \psi} = -\frac{3}{2} \sin(2\psi)$, and evaluating at $\psi = \epsilon$, the tidal lag angle between the star's tidal bulge and the star-planet axis.

5. The tidal lag angle arises because material in the star, even if it is perfectly elastic, may be viscous, meaning it cannot immediately change shape due to frictional forces between particles. Assuming the stellar interior behaves like a Kelvin-Voigt material, its response to a periodic driving force can be modelled as a forced harmonic oscillator of the form:

$$\frac{d^2x}{dt^2} = -\omega_0^2 x - \frac{1}{\tau} \frac{dx}{dt} + \frac{F_0}{m} \cos \omega t$$

Where:

- ω is the frequency of the driving force i.e. the orbital frequency minus the star's rotational frequency
- ω_0 is the natural frequency of the star,
- x is the displacement of particles from equilibrium due to tidal forcing.

The first term represents simple harmonic oscillation of a bulge around a “natural frequency” with which the star redistributes material. The second term represents a dampening due to frictional forces that slow the movement of material. The final term represents the external gravitational driving force producing the tidal bulge.

6. The forced harmonic oscillator gives a solution of the form:

$$x = A \cos(\omega t + 2\epsilon)$$

$$\sin 2\epsilon = -\frac{\omega}{\tau} \left[(\omega_0^2 - \omega^2)^2 + \left(\frac{\omega}{\tau}\right)^2 \right]^{-\frac{1}{2}}$$

If the damping is weak, $\left(\frac{\omega}{\tau}\right)^2 \ll \omega^2, \omega_0^2$:

$$\sin 2\epsilon \propto \frac{1}{\omega_0^2 - \omega^2}$$

If the natural frequency of the star is significantly greater than the orbital frequency, $\omega^2 \ll \omega_0^2$, then the tidal lag has constant phase delay:

$$\sin 2\epsilon = \text{const.}$$

In the case of hot Jupiter systems orbital frequencies are significantly lower than most resonant frequencies of the star. If we neglect the frequency dependence of damping term the above simple relationship holds. However, the causes of damping in stars and their natural frequencies are not entirely well understood, so care must be taken. As a cautionary tale: George Darwin's assumption of a constant phase lag caused him to underestimate the Moon's age by a factor of four.

7. The lag can be shown to relate to the specific dissipation function Q of the oscillator, defined as the ratio of the peak energy stored during a single cycle of the oscillator over the energy dissipated during a cycle:

$$Q = \frac{2\pi E_0}{\Delta E} = \frac{1}{\sin(2\epsilon)}$$

Giving the following condensed expression for the torque experienced by the planet:

$$T = -\frac{3}{2} \frac{GM_p}{a} \left(\frac{R}{a}\right)^5 \frac{k}{Q}$$

Since the properties of the Love number and Q cannot be separated by simple transit observations, the two properties are usually grouped together into a single property known as the “modified stellar tidal dissipation factor”.

$$Q' = \frac{Q}{k}$$

8. The work done by the torque decreases the orbital energy of the planet:

$$\dot{E} = T(\omega - n)$$

Where n is the mean angular velocity of the planet and ω the star’s rotational velocity.

9. The total energy of the system (which is not conserved due to heating/friction as the tidal bulge moves across the star):

$$\begin{aligned} E &= \frac{1}{2} I \omega^2 - \frac{1}{2} \frac{GM_* M_p}{a} \\ \dot{E} &= I \omega \dot{\omega} + \frac{1}{2} \frac{GM_* M_p}{a^2} \dot{a} \\ &= I \omega \dot{\omega} + \frac{1}{2} n^2 a \dot{a} \frac{M_* M_p}{M_* + M_p} \end{aligned}$$

Where Kepler’s third law gives: $n^2 = \frac{G(M_* + M_p)}{a^3}$

10. Total angular momentum of the system (which is conserved):

$$\begin{aligned} L &= I \omega + \frac{M_* M_p}{M_* + M_p} n a^2 \\ \dot{L} &= I \dot{\omega} + \frac{1}{2} \frac{M_* M_p}{M_* + M_p} n a \dot{a} = 0 \end{aligned}$$

Where the moment of inertia of two point particles is given by: $I = \frac{m_1 m_2}{m_1 + m_2} a^2$

11. Combining these four equations yields the oft-quoted stellar tidal decay equation:

$$\begin{aligned}\dot{a} &= \text{sign}(\omega - n) \frac{3}{Q'} \frac{M_p}{M_*} \left(\frac{R_*}{a} \right)^5 na \\ &= \text{sign}(\omega - n) \frac{3}{Q'} \sqrt{\frac{G}{M_*}} M_p R_*^5 a^{-\frac{11}{2}}\end{aligned}$$

which agrees up to a constant of proportionality with a fuller derivation quoted by Jackson et al (2008) [16].

This equation relates change in semi-major axis (the “decay rate”) to the masses of planet and star, stellar radius, semi-major axis, and most importantly the modified stellar tidal dissipation factor, which as discussed encodes information about the rigidity, elasticity and viscosity of the body.

Consequently, tidal decay is linked to stellar composition and structure and decay rates provide information about what the star is made of. There are similar effects due to tides raised by the star on the planet, but in practice these are an order magnitude smaller.

Since the equation presented is proportional to the mass of the planet and inversely proportional to a large power of semi-major axis, it is clear that decay rates should be most pronounced in large, close-in planets such as hot Jupiters. The most famous and only confirmed example of such decay is WASP-12b which has both a large mass ($1.5 M_J$) and small semi-major axis (0.024 AU) [33]. It will be discussed further in section 2.3.2.

Note that the derivation assumes zero eccentricity. A more comprehensive analysis accounting for eccentricity yields a coupled differential equation in both \dot{a} and \dot{e} . However, the simpler solution derived above will be acceptable in this project as hot Jupiters typically have low eccentricity, likely due to years of tidal circularization having run its course as discussed in section 2.3.1.

2.3 How can tidal decay be observed?

There are two different approaches to observing tidal decay experimentally.

2.3.1 Statistical approaches

Indirect evidence for tidal decay comes from comparing the observed distributions of orbital parameters of known exoplanets to the expected distribution of those parameters under tidal evolution models. In particular, comparing the age distribution of close-in planets to that of wider-orbit planets, or analogously, the distribution of semi-major axis around young stars to that of older stars.

For example, in their 2008 paper, Jackson et al compared the distribution of close-in exoplanets of semi-major axis < 0.2 AU with the larger sample of wider-orbit planets > 0.2 AU. They noted the eccentricities of close-in planets were on the whole smaller than that of further out planets, and attribute this observation to the effect of tidal circularization over time [16].

Using estimates of the age of host stars as a proxy for the age of the planets, they integrated out the differential equations described in section 2.2 over the lifespan of the stellar systems in question. This produced an initial distribution of semi-major axes and eccentricities that could then be compared to the current distribution of wider-orbit planets. Assuming that the close-in planets all evolved from an initial set of wider orbits, one can fit the tidal dissipation factors to equate the two distributions together. Jackson et al found the value of stellar tidal dissipation factors to lie around $10^{5.5}$.

Meanwhile Pont (2009) and Husnoo et al (2012) provide evidence of hot Jupiter-hosting stars spinning faster than usual, suggesting a transfer of angular momentum has taken place due to tidal decay [30] [13]. In fact several stars including KELT-1 exhibit a spin consistent with tidal synchronization between star and planet [31].

Tidal decay has been invoked more recently to explain the observed paucity of planets with very small semi-major axes: these planets’ orbits may have decayed so much they reach their “Roche” limit, the point at which the star’s tidal forces overcome the planet’s self-gravitation and tear it apart [15]. Whilst most systems are expected to evolve towards a state of tidal equilibrium in which the planet is in a synchronous orbit with the star’s spin, Ogilvie (2014) points out that in systems of extreme mass ratio, tidal equilibrium cannot be reached. Instead, the orbit shrinks until the planet is destroyed [27].

Similar arguments can be extended to provide bounds of tidal dissipation factors for highly-eccentric systems. Hansen (2010) constrained tidal dissipation factors by arguing that high tidal energy dissipation would not allow for highly eccentric yet reasonably old systems to survive to the present day: they should have circularised or decayed long ago. Therefore upper bounds may be placed on the tidal dissipation rates of highly-eccentric short-period exoplanets like WASP-17b, which has eccentricity $e = 0.13$ [11].

However such statistical analyses rest on a set of somewhat unrealistic assumptions:

- All stars share the same tidal dissipation factor. In reality stars come in many shapes and sizes and their interiors vary wildly. The dissipative processes occurring in red giants are unlikely to be entirely comparable to the dissipative processes occurring in main sequence stars.
- All planets within a particular value of semi-major axis have evolved from initial positions further out. Whilst it is theorised that larger planets are more easily formed further away from their host stars, smaller planets may have formed in this band. Indeed less massive planets undergo less tidal decay as seen in equation x, so it is less likely small planets evolved from positions further out.

2.3.2 Direct observation

In contrast to the statistical methods discussed, we can directly observe decay by monitoring the change in orbital period of a planet over time. This is usually done with transit timings because transit observations are plentiful as discussed in section 2.1. This approach does not make assumptions about tidal dissipation factors or orbital evolution. Instead, we can actually directly infer the value of tidal dissipation factors for a single system and measure its semi-major axis decay rate.

Space or ground based telescopes record the light flux received from a star using a CCD imaging sensor. The light flux is integrated over a given sampling interval (2

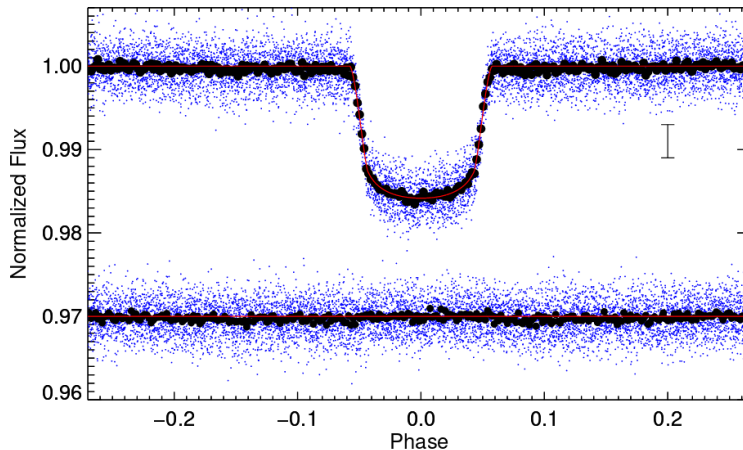


Figure 3: Phase-folded transit light-curve from TESS observations of WASP-12b [33].

minutes for most TESS targets [32]) to give a time series of flux with a given sampling resolution. A dip in this flux could result from a planetary transit and is known as a “transit light curve”.

Such periodic dips in flux can be identified by algorithms like the discrete Fourier transform (DFT) which will extract out the spectra of frequencies present in the signal. More common these days however is the box least-squares periodogram (BLS) introduced by Kovacs et al in 2002. This method fits box-shaped functions to the data as opposed to sinusoids like a DFT, resulting in better fits since the actual shape of transit light curves tend to be “boxy” [21].

Once individual transits are identified, the shape of the transiting light curve can be modelled more finely using numerical MCMC methods and software packages like BATMAN [22]. The shape depends on the planet’s semi-major axis, inclination, eccentricity and radius, and the resulting fit provides the transit “mid-time”, the time at which the planet is in full conjunction with the Earth-star axis and at which the light curve reaches its greatest depth.

Several such transit light curves may be individually or simultaneously fitted to produce a sequence of transit times. The differences between these transit times is usually a constant period, but may decrease if the planet’s orbit is slowly decaying. Figure 3 shows an example of fitting a light-curve to light flux observations that have been phase-folded assuming a constant period.

The differences in transit times are so small that they are usually plotted residualised against a constant period model fit. These residuals are often referred to as “transit timing variations” (TTVs) or “observed-computed” times. An example of such a plot is shown in Figure 4 overlaid with lines representing the best-fit orbital decay and apsidal precession models.

The decay effect can be modelled by considering the transit times as a function of orbit number (referred to as epoch E):

$$T(E) = \int dt = \int \frac{dt}{dE} dE = \int P(E) dE$$

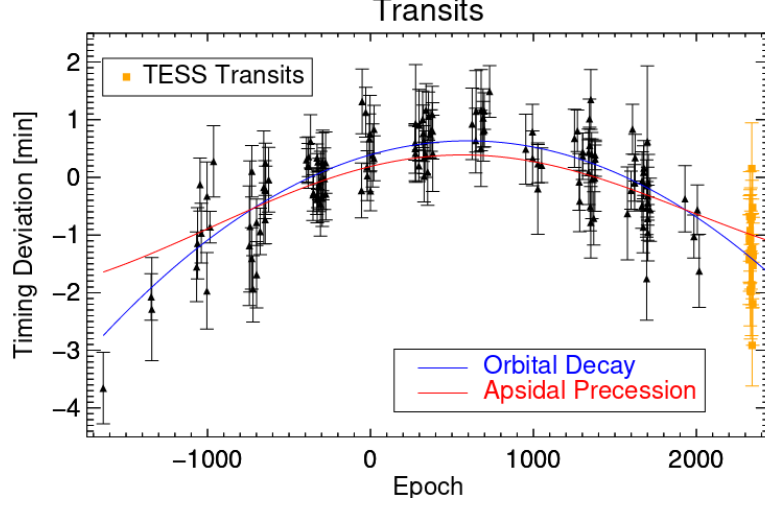


Figure 4: Transit timing variations from TESS observations of WASP-12b [33].

Where the period P as a function of orbit number E can be Taylor expanded as follows:

$$P(E) = P_0 + \frac{dP}{dE}E + \frac{1}{2} \frac{d^2P}{dE^2}E^2 + \dots$$

Using Kepler's third law:

$$\begin{aligned} 4\pi^2 a^3 &= GM_* P^2 \\ \Rightarrow a &= \left(\frac{GM_*}{4\pi^2} \right)^{\frac{1}{3}} P^{\frac{2}{3}} \\ \Rightarrow \dot{a} &= \frac{2}{3} \left(\frac{GM_*}{4\pi^2} \right)^{\frac{1}{2}} P^{-\frac{1}{3}} \dot{P} \end{aligned}$$

We can substitute into the tidal decay equation (11) to show that second order terms of $P(E)$ are negligible:

$$\begin{aligned} \frac{2}{3} \left(\frac{GM_*}{4\pi^2} \right)^{\frac{1}{2}} P^{-\frac{1}{3}} \dot{P} &= -\frac{3}{Q'} \sqrt{\frac{G}{M_*}} M_p R_*^5 \left[\left(\frac{GM_*}{4\pi^2} \right)^{\frac{1}{3}} P^{\frac{2}{3}} \right]^{-\frac{11}{2}} \\ \Rightarrow P^{\frac{10}{3}} \frac{dP}{dt} &= \text{const.} \\ \Rightarrow P^{\frac{7}{3}} \frac{dP}{dE} &= \text{const.} \\ \Rightarrow \frac{d}{dE} \left(P^{\frac{7}{2}} \frac{dP}{dE} \right) &= 0 \\ \Rightarrow \frac{d^2P}{dE^2} &= -\frac{7}{3} \frac{1}{P} \left(\frac{dP}{dE} \right)^2 \ll \frac{dP}{dE} \end{aligned}$$

Consequently transit times are modelled as:

$$T(E) = \int P(E)dE \approx T_0 + P_0 E + \frac{1}{2} \frac{dP}{dE} E^2 + \epsilon$$

Where ϵ represents an additional noise term due to measurement inaccuracies, which is assumed to be distributed normally with some error $\epsilon \sim N(0, \sigma^2)$. This model is sometimes referred to as the “quadratic ephemeris” model due to its dependence on the second power of epoch E .

From this model we wish to infer the reference transit time T_0 , the reference period P_0 and the decay rate per epoch $\frac{dP}{dE}$. This can be done using maximum likelihood estimation, but more frequently a full Bayesian method is used which has the key advantage of also estimating the uncertainty in each of the fitted parameters.

Most commonly, Monte Carlo Markov Chain estimation is used. This is a technique that sequentially samples from the parameter space. At each step it evaluates the posterior distribution at this point and uses the result to inform its selection of the next point in the space to sample. When the autocorrelation of posterior evaluations reaches a particular threshold the sampling chain is said to have converged and the fit is complete.

Examples of this methodology in action can be found in the work of Hagey et al (2022), Ivshina and Winn (2022), Patra et al (2020) and Turner et al (2021). In these papers the authors all study the transit timing variations of WASP-12b, a close-in hot Jupiter exoplanet with an orbital period of 1.09 days. All four authors use an MCMC method to fit the quadratic ephemeris model to a series of transit times but using slightly different data: Ivshina & Winn and Turner make use of TESS data whilst Hagey supplements TESS data with citizen-scientist data collected by the Exoplanet Transit Database and Patra presents some proprietary ground-based measurements of their own.

The papers agree that there is strong evidence that WASP-12b is decaying according to the quadratic ephemeris model with a period decay rate of approximately 0.08 ms/epoch or, at the current length of an epoch, 30 ms/year. From this decay rate and the tidal decay equation (11), Turner infers a modified stellar tidal dissipation factor of $1.39 \pm 0.15 \times 10^5$ for WASP-12b’s star. This decay is extremely small, and far below TESS’ maximum photometric sampling rate of 20s, but the second order term in the quadratic ephemeris model shows that decay increases with time by order $O(t^2)$. A 0.08 ms/epoch decay rate actually compounds to a variation of $\frac{1}{2} \frac{dP}{dE} \frac{t^2}{P_0^2} \sim 300s$ over a ten year period - a magnitude that should clearly be visible in transit observations with TESS.

2.4 How can confounding factors be ruled out?

It is difficult to be entirely sure of the presence of tidal decay when there are so many confounding factors at work. As discussed in section 1.2, several physical phenomena could effect changes in a planet’s orbit and under circumstances be mistaken for tidal decay.

In particular:

- The perturbing gravitational potential of companion planets may cause precession and produce additional tidal behaviour in the transiting planet. A good example of such a system is TOI-270, a system with three planets in mean-motion resonance

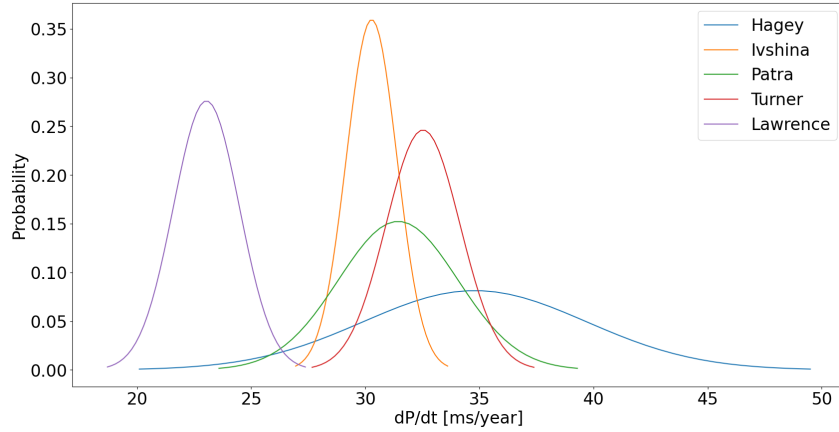


Figure 5: Posterior distributions over WASP-12b’s decay rate published in the literature.

(their periods being integer ratios of each other). Kaye et al note that this resonant behaviour produces large transit timing variations and use these variations to constrain the masses and eccentricities of the planets with much more confidence than is usually possible in non-resonant non-interacting transiting planets [19].

- Massive, wide-orbiting companions can cause line-of-sight accelerations of the transiting planet-star system which cause transit frequencies to vary in a similar manner to a Doppler shift. Bouma et al identify this as a likely explanation for the transit timing variations of WASP-4b [4].
- Stellar activity may introduce noise into the photometric light flux readings taken by telescopes. The brightness of stars may oscillate over time, but the appearance and movement of stellar spots over time are often more problematic. A planet transiting such a spot will produce a noticeably smaller transit depth signal than without the spot and this can alter the shape of the light curve. In the case of WASP-10b’s observed transit timing variations, Barros et al refute Maciejewski et al’s earlier hypothesis that the planet has a wide-orbiting companion and have instead presented new transits and models that suggest stellar spots combined with incorrect data normalization are to blame [3].
- Active stars may become more and less oblate over their activity cycles due to magnetic torques, something called the Applegate effect [1]. The oblateness creates a perturbing potential which can cause planetary orbital decay in much the same way as a tidal bulge. Watson et al identify WASP-18b as a planet whose transit timing variations are equally well explained by a perturbing companion planet or the Applegate effect [34].
- Inhomogeneous data processing and normalization such as inhomogeneous fitting of light-curves. There are different techniques for doing so and different methods may produce systematically different mid-transit times. Judkovsky et al conclude in a recent 2023 paper that a fitting process relying directly on homogeneous flux fitting should be preferred to one that draws mid-transit times from inhomogeneously fitted sources [17].

- Experimental precision also limits the accuracy of transit time measurements: there is a fundamental lower limit due to the sampling intervals over which the light flux is integrated (20s for TESS targets). The precision may be even worse for ground-based telescopes due to the impacts of atmospheric turbulence and stray light. Whilst more data over a longer timespan is useful for observing slow-moving phenomena like tidal decay, lower quality observations must be handled with caution. Hagey et al made use of citizen-scientist transit observations from the Exoplanet Transit Database in their 2022 TTV survey, but noted that they were only able to achieve sensible results in planets with more than 80 contributed transit observations - implying that a handful of outliers existed which distorted the results. Some of these may not even be real transits [10].

A few approaches are used in the literature to try to overcome these limitations and determine the cause of transit timing variations with greater certainty:

1. Noisy measurements can be eliminated using outlier rejection techniques. Ivshina & Winn discarded datapoints whose residual to a constant period fit was more than an arbitrary magnitude, as well as adding a jitter term to their model to account for systematic errors in their data [14], whilst Hagey et al used an iterative sigma-clipping method in which they repeatedly discarded datapoints more than three standard deviations away from their model’s fit until no such “erroneous” datapoints remained [10].
2. Different models can be tried and their strength of fit assessed by testing the normality of the residuals: after all, the model assumes errors are normally distributed. This is known as the χ^2 test since the sum of normally distributed residuals should be χ^2 -distributed. Alternatively, statistical criterion such as the Bayesian Information Criterion can be used which better account for the degrees of freedom available in more complex models. Turner et al used these metrics when fitting transit timing variations in their 2020 investigation of WASP-12b. They tried a constant period model (no decay), the quadratic ephemeris model and an apsidal precession model. The χ^2 and BIC metrics both favoured the quadratic ephemeris model leading them to conclude that WASP-12b is decaying [33].
3. More data can be used, as Hagey et al noted in their 2022 paper [10]. The effect of a handful of large outliers is reduced the more non-outlying data we have available: if outliers are present in a dataset with uniform probability, then the smaller the dataset, the more likely an extreme fraction of the dataset is erroneous.

2.5 How does stellar structure relate to tidal decay?

In the derivation of tidal decay theory in section 2.2 two parameters were derived: the potential Love number k which encapsulates the magnitude of the tidal bulge due to rigidity and elasticity of the star, and the tidal dissipation factor Q which describes how material in the star moves in response to an oscillating driving force.

The apparent simplicity of these two parameters belies a much more complicated system. In reality, if the perturbing body has non-negligible orbital eccentricity or inclination, then the tidal potential (which we previously approximated with a binomial

expansion) has many components, each of which drives the distortion of material in the planet at a particular frequency. In addition, the damping term presented is not necessarily negligible and therefore the response of the star to the tidal potential is not frequency-independent. As a result, Goldreich (1963) and Greenberg (2009) both point out that Q is not fixed for a given body - it is in fact strongly dependent on the frequency of the driving potential, where this driving potential itself may consist of many frequency components [7] [9].

The simplified model we have considered so far is solely that of the equilibrium tidal potential induced by a zero-eccentricity perturbing body whose orbital axis is aligned with the star’s rotational axis. Nevertheless such a simplified model can yield some insights into the stellar interior. Theoretical estimates of the tidal dissipation factor Q can be computed from physical models of how energy is stored and dissipated in a star distorted by a perturbing planet.

In the limit where tidal forcing frequency is suitably small, we can assume the star remains in hydrostatic equilibrium. The density and pressure can then be directly related to the amplitude of tidal displacement. Solving for this amplitude is degenerate because the Love number k cannot be separated from tidal dissipation factor Q , but if it could, one would have an extra equation relating pressure and density with which to constrain the traditional Lane-Emden equation of stellar modelling [27].

As discussed, the equilibrium tide involves a flow of material and any process resisting this flow leads to dissipation of energy. Ogilvie notes that molecular viscosities are too small to cause dissipation and the main cause is rather turbulence in the convective zones of stars (the region of a star in which energy is transported predominantly by means of convection due to large temperature gradients). A classic approach to characterizing the dissipation of energy in a turbulent fluid is to calculate an effective “eddy” viscosity. The larger the eddy viscosity the larger the rate of tidal dissipation. The effective eddy viscosity also scales with the mass of the convective zone, so in theory knowledge of the tidal dissipation factor could be used to constrain the mass of convective zones if one assumes that the primary cause of tidal dissipation is turbulent eddy viscosity.

Beyond the equilibrium tide, there is also a wave-like dynamic tidal response in the star due to internal gravity and inertial waves, which are expected to be more important at higher forcing frequencies. Oscillation modes of stars have already been widely studied for the purpose of asteroseismology (inferring structure through oscillations in stellar brightness), but tidal forcing frequencies are typically much lower than the surface gravity and acoustic pressure waves that asteroseismology considers. The study of gravity and inertial waves in stars is still a developing field. These waves are very different in the radiative versus convective zones of a star, and dissipation of energy is only effective at lower tidal forcing frequencies than is typical in hot Jupiter systems.

3 Conclusion

Observational study of the evolution of exoplanetary orbits is a young field that has only recently become possible thanks to the large scale transit surveys performed by Kepler and TESS and the contributions of a large number of citizen-scientist observations. There remain a number of open problems that my project seeks to address.

3.1 Goals

The goals of this project are to:

1. Identify hot Jupiters with statistically significant transit timing variations (TTVs) that are good candidates for follow up study for signs of tidal decay.
2. Develop a rigorous statistical methodology for modelling tidal decay in these systems, accounting for experimental errors and disentangling other TTV inducing phenomena.
3. For those systems undergoing tidal decay, measure and classify the strength of tidal dissipation by stellar age and position on the main sequence, and use the resulting distribution over tidal dissipation factors to test and inform models of stellar structure, in particular the mass and depth of the convective zone.

In particular, I will focus on tackling the following open problems:

1. Empirical analysis of the distribution of tidal dissipation factors.

So far, studies have mostly concentrated either on a small handful of systems, or applying statistical techniques like Jackson (2009). Hagey et al (2022) have made use of citizen-science data for 400 planets, and Ivshina & Winn (2022) have modelled TESS observations of 382 planets, but a comprehensive study ought to collate all available data together to produce the most thorough survey possible and best constrain decay rates [10] [14]. This is the first milestone aim of my project.

Furthermore, a wide scale survey of orbital decay will allow us to construct the empirical distribution of decay rates and tidal dissipation factors from which statistical analyses can be performed. In particular, it will be interesting to study how the tidal dissipation factors of stars relate to other stellar properties. What might we understand by analysing a large sample of planets rather than just individual planets?

2. Connecting tidal dissipation factors with modelling of stellar interiors.

In theory, the stellar tidal dissipation factor is a property determined by stellar composition and structure. Most observational research papers end with a computation of the tidal dissipation factor, but there is a significant body of work by Goldreich, Ogilvie and others that studies tidal responses in stars and planets in detail. That work has largely focused on theory and observations within our solar system - my project aims to test it in the context of real exoplanet observations.

Such theoretical modelling of tidal responses could also be used as a new tool with which to study stellar interiors, and, with high enough observational precision, planetary interiors. Ogilvie (2014) suggests that future work ought “to take into account the dependence of tidal response on the extent of the stellar convective zone”. In conjunction with observations of tidal decay this could help us better constrain the extent of convective zones, which are supposed to depend on the star’s mass and its evolutionary phase. Solar-like stars are theorised to have convective envelopes around radiative cores, but higher mass red giants are supposed to have

convective cores. Observational evidence through tidal responses could help pin down these relationships and validate our understanding of stellar evolution and structure [27]. In particular, I will focus on understanding the relationship between stellar convective mass and tidal dissipation factors.

3. Improving statistical methodologies.

Current transit timing variation modelling in the literature suffers from a number of problems.

- (a) Differing and inconsistent methodologies. This makes it hard to compare and collate results across papers, particularly when the papers investigate planets with no overlap. Ideally a homogeneous analysis should be performed before reasoning about any empirical distributions that result.
- (b) Biased outlier detection methods. Various forms of outlier detection are used to improve the quality of the dataset being used and remove datapoints which may be false positives or have significantly higher than reported error. The most common form of detection used involves fitting a decay model to all the data and excluding datapoints which do not agree to this fit to within some standard deviation threshold. This type of “parametric” outlier detection, so called because it parameterises the model, results in a biased final dataset, as points which do not agree with the assumptions of the model have been discarded. Hagey et al (2022) acknowledge this shortcoming and justify it by performing the same outlier detection with another model and confirming that the final results are similar. Despite the justification the method leaves a lot to be desired: in my project I will aim to develop more robust methods.
- (c) Different papers sometimes reach inconsistent results due to use of different data. Ideally analysis should be performed on a super-set of all available public data. Even when not, the results should be consistent: more data should only lead to a stronger confidence in evolutionary parameters like decay rate.

To this end, I will aim to assemble a more comprehensive dataset than previous studies have used, including photometric data from Kepler and TESS and citizen-scientist observations from the Exoplanet Transit Database and ExoClock. TESS’ all-sky coverage and continuing operation means there is a rapidly growing dataset with which to work and build upon existing research. Meanwhile, though lower quality, the citizen-scientist datasets help extend the time range baseline of observations outside of TESS and Kepler’s observing windows.

Pre-fitted mid-transit times will be used, since these are more likely to be publicly available and fitting light-curves is particularly computationally expensive. We will assume that fitted transit mid-times are unbiased and distributed with Gaussian error (something which is contested by Judkovsky et al (2022) but will nevertheless greatly simplify the modelling process).

- (d) Because of the relatively high noise to signal nature of the problem, it is important to model the uncertainty in fitted parameters like decay rate. As a result Bayesian modelling methods are used nearly universally. However, most

papers make use of Markov Chain Monte Carlo, a class of numerical methods for performing Bayesian inference. These methods are typically slow and CPU intensive. In addition they are not guaranteed to converge (indeed convergence becomes extremely difficult for high dimensional models), and MCMC methods cannot compute the Bayesian model evidence (a statistical gold standard for model comparison) meaning approximations like the Bayesian Information Criterion (BIC) must be used to compare different model fits.

This overuse of MCMC overlooks the fact that models can often be formulated that are linear in the parameters, meaning well-understood, fast, analytical methods from the field of Bayesian multivariate regression can be used instead. In contrast to the literature, in this project I will aim to develop such an analytical fitting procedure in order to speed up and improve the robustness of TTV modelling. As is common in the literature, we will use χ^2 to check normality of residuals and the BIC to compare models but I will also attempt to construct the true model evidence as is favoured in Bayesian statistics.

- (e) Tidal decay modelling typically assumes a quadratic ephemeris which comes from Taylor expanding to second order. Whilst higher orders should be negligible, there does not appear to be a good reason for why those orders must be neglected. In theory, the full tidal decay equations could be integrated relatively trivially to get a non-approximated model that transit times can be fitted to. In this project we will initially model transit times according to the quadratic ephemeris model, and later attempt to extend the model beyond the second order approximation discussed.

4. Rigorously examining and ruling out other TTV inducing phenomena.

Most papers are plagued with uncertainty about whether systems are tidally decaying or exhibiting transit timing variations that are the result of another phenomena, like precession due to a perturbing companion planet, line-of-sight acceleration due to a wide, massive orbiting companion or the Applegate effect.

A rigorous process for examining all these cases and ruling them out needs to be developed before we have a hope of examining tidal decay en-masse without significant and time-consuming analysis of individual systems.

This is a relatively tricky and degenerate problem to solve and in the interests of time will not make up a significant chunk of my project. Instead, I will assume that stellar tidal decay is the dominant cause of transit timing variations, and that other physical effects are either sufficiently small or sufficiently uncommon so as to be negligible when sampling many planetary systems at once. This should be reasonably true: resonant multi-planet systems are relatively uncommon (though their effects on TTVs can be large), whilst other effects like stellar oblateness tend to be small. We will also assume that the effect of tides raised on the planet is orders of magnitude smaller due to the low mass of the planet. My thesis will discuss the validity of these assumptions in more depth.

5. Formulating observational strategies.

There are as of yet no published studies that have compiled a thorough list of objects of interest for the study of tidal decay. In addition, no observation plan has been put forward for how to best study a set of planets that might be decaying. With multiple transit observing exoplanet missions like PLATO and ARIEL set to launch in the next few years, it would be prudent for researchers interested in this field to assemble a consistent proposal for observing time.

In my project, theoretical predictions of tidal decay, combined with current observations, will be used to create a ranking of interesting planetary candidates. Those candidates will be narrowed yet further according to whether new observations reduce the posterior uncertainty enough to classify the decay of the system. Finally, a coherent observational strategy will be established: how often and with what cadence should a particular system be observed, and if observations are constrained, should we focus on collecting more transits for fewer planets, or fewer transits for more planets?

3.2 Preliminary results

To start with, I have created a ranking of promising tidal decay candidates according to the magnitude of their predicted decay under the equation derived in section 2.2. The ranking assumes a value for the tidal dissipation factor of the star equivalent to that reported for WASP-12 ($\sim 10^{5.5}$) and uses planetary data collected by the NASA Exoplanet Archive [26]. Out of 4760 planets for which we were able to compute a prediction, 25 had a predicted decay rate in excess of 25 ms/year, including several candidates known to exhibit transit timing variations according to the literature, including WASP-12b, WASP-18b and HATS-18b.

We see in Figure 6 that the largest predicted tidal decays are on the order of 100 ms/year, and the effect of stellar tides on the decay rate is typically an order of magnitude more prominent than the effect of planetary tides. This provides a rough justification for one of our initial assumptions: that decay due to stellar tidal dissipation dominates that of planetary tidal dissipation. Similar analysis shows that whilst the full tidal decay equations are sensitive to eccentricity, the length of the semi-major axis is much more important. For close-in exoplanets that are already on near-circular orbits, the approximate tidal decay equation derived in section 2.2 will be more than adequate. Further work will augment these predictions to construct an overall ‘observability’ ranking that accounts for both magnitude of predicted decay, and how likely we are to be able to constrain that orbital decay with a given set of additional measurements.

Subsequently, I have developed a Bayesian linear regression fitting method as discussed in section 3.1 and applied it to real transit observations collected by the Exoplanet Transit Database [6]. To start with, I applied the method to transits of WASP-12b. The resulting residualised transit timing variations are shown in Figure 7. It is evident from the shaded orange area (representing the model’s 3 standard deviation uncertainty) that the model favours a decaying orbital period as opposed to a constant orbital period. The resulting decay rate of 0.06 ms/year is slightly inconsistent with corresponding literature values, as shown in Figure 5.

Perhaps unsurprisingly, this is caused by outliers in the citizen-scientist data the ETD collates. When re-fitting using the same data as Turner et al (2021), the method finds con-

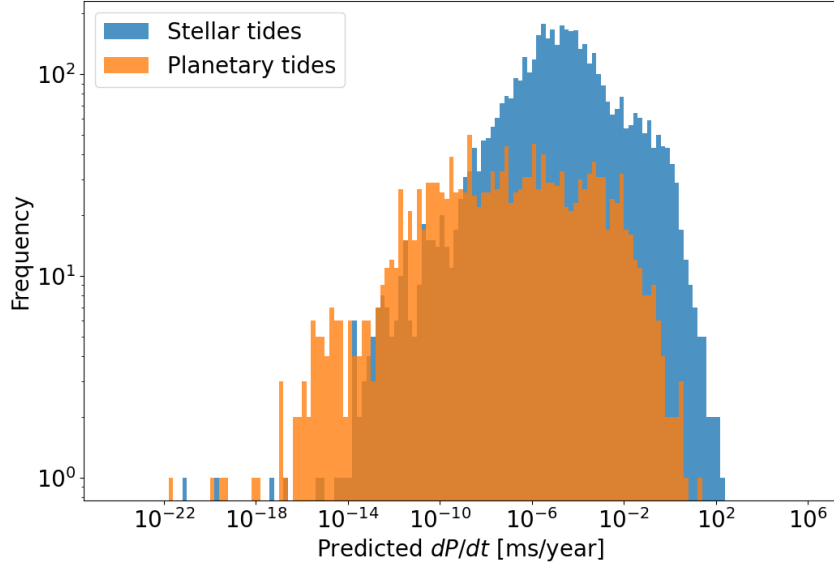


Figure 6: Distribution of predicted decay rates for stellar and planetary tidal interactions.

sistent values of 0.08 ms/epoch, but using the faster and more robust analytical approach I have developed. Results for several other planets and a comparison to corresponding results from the literature are shown in Figure 8. In some cases my results agree closely, in some they do not. Beyond the inconsistencies due to data quality, further work is required to understand these differences more carefully.

Finally, the predicted decay rates have been combined with the fitted observational results discussed to create a plot of observed decay rates vs theoretical decay rates in Figure 9. The ETD data has been supplemented by TESS transits collated by Ivshina and Winn (2022) and more citizen-scientist transits collated by ExoClock [20].

WASP-12b sits neatly on the green line where theory matches observation. Other planets with a high probability of decay whose observations match theory include TRES-3b, WASP-4b and WASP-18b. These would be good candidates for further observation. However, a good number of planets appear to exhibit decay rates far outside what is expected under theory. This could be due to incorrect assumptions in the theoretical predictions. For example, we assumed that all stars had a similar tidal dissipation factor to WASP-12a. It could also be due to confounding physical effects like resonant multi-planet systems that can sometimes look like decay. Further work is required to weed out these anomalies before we can relate these decay rates to stellar tidal dissipation factors with confidence.

3.3 Summary

The search for and characterisation of extra-solar planets is a rapidly developing field with wide implications for the study of stellar and planetary formation, evolution and structure. What was once a small sample of known exoplanets has grown into a populous cosmic zoo of hot-Jupiters, sub-Neptunes, super-Earths and others. Much of this can be attributed to the success of transit observing space telescopes like Kepler and TESS.

In particular deviations in transit times of exoplanets from what might be expected

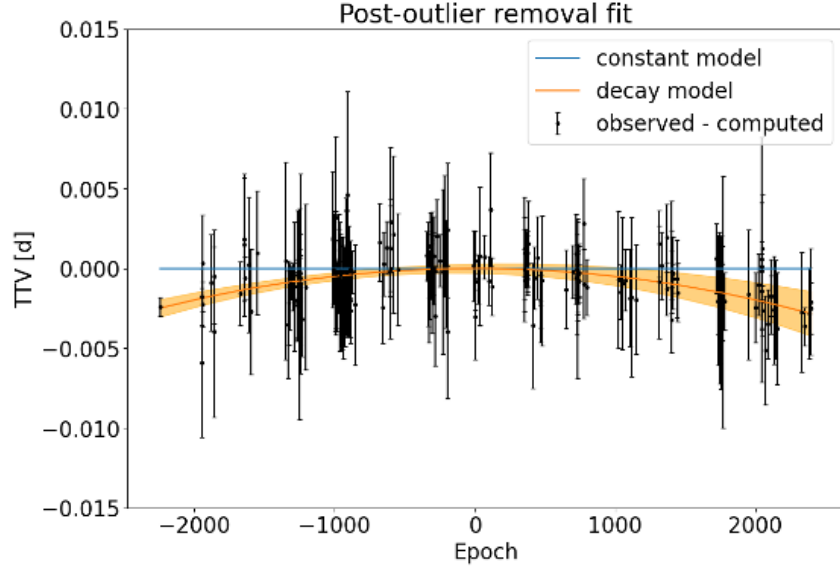


Figure 7: Transit timing variations of WASP-12b. Each point represents a transit time, residualised against the time we would expect under the assumption of a constant period. This is sometimes also referred to as ‘observed - computed’ times.

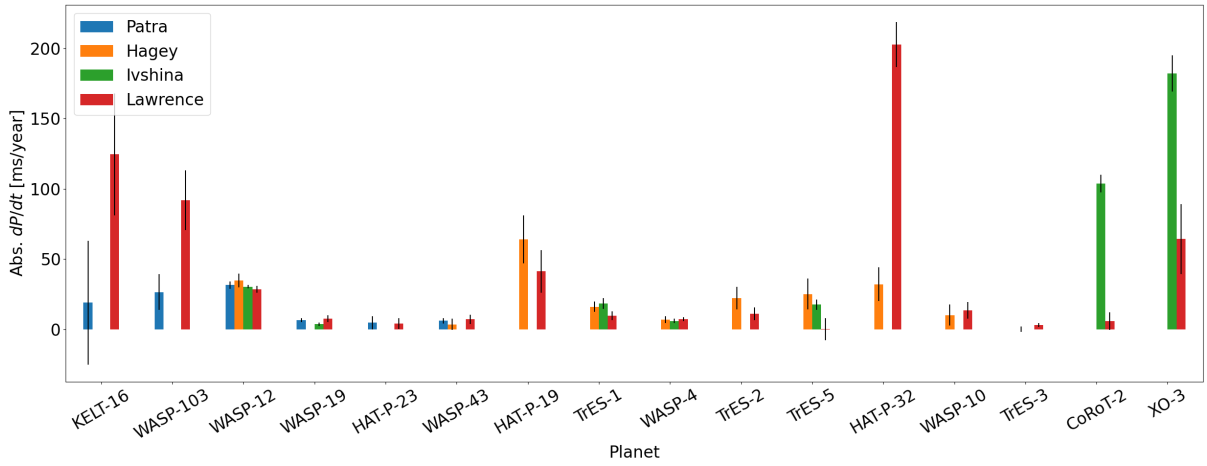


Figure 8: Fitted decay rates of several planets compared to literature values.

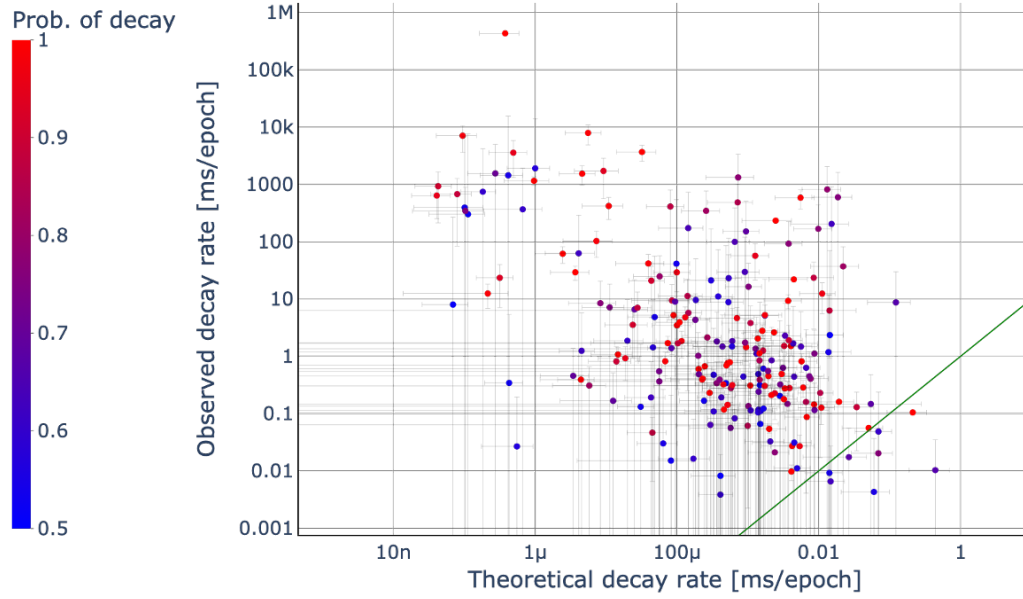


Figure 9: Observed vs theorised decay rates for a sample of 400 planets. Red points indicate planets with a high probability of decay under the model, and blue low probability of decay.

under the assumption of a constant period orbit (transit timing variations) can be used to study how planetary orbits evolve over time, due to effects such as multi-planet resonances, stellar oblateness and tidal interactions. It is the latter effect which this project intends to study: principally, how such tidal interactions lead to orbital decay and what this could tell us about stellar structure and the extent of a star’s convective zone. We will use transit timing variations to identify systems undergoing tidal decay, investigate the relationships between tidal decay and host stars, and develop an understanding of how such decay relates to stellar structure. Finally, the observations could prove a valuable test of tidal interaction theories proposed by the likes of Ogilvie et al.

References

- [1] James H. Applegate. “A Mechanism for Orbital Period Modulation in Close Binaries”. In: *The Astrophysical Journal* 385 (Feb. 1, 1992). ADS Bibcode: 1992ApJ...385..621A, p. 621. ISSN: 0004-637X. DOI: 10.1086/170967. URL: <https://ui.adsabs.harvard.edu/abs/1992ApJ...385..621A> (visited on 03/01/2024).
- [2] S. C. C. Barros et al. “Detection of the tidal deformation of WASP-103b at 3σ with CHEOPS”. In: *Astronomy & Astrophysics* 657 (Jan. 2022), A52. ISSN: 0004-6361, 1432-0746. DOI: 10.1051/0004-6361/202142196. arXiv: 2201.03328[astro-ph]. URL: <http://arxiv.org/abs/2201.03328> (visited on 02/22/2024).
- [3] S. C. C. Barros et al. “Transit timing variations in WASP-10b induced by stellar activity”. In: *Monthly Notices of the Royal Astronomical Society* 430.4 (Apr. 21,

- 2013), pp. 3032–3047. ISSN: 0035-8711. DOI: 10.1093/mnras/stt111. URL: <https://doi.org/10.1093/mnras/stt111> (visited on 03/01/2024).
- [4] L. G. Bouma et al. “WASP-4 Is Accelerating toward the Earth”. In: *The Astrophysical Journal* 893 (Apr. 1, 2020). ADS Bibcode: 2020ApJ...893L..29B, p. L29. ISSN: 0004-637X. DOI: 10.3847/2041-8213/ab8563. URL: <https://ui.adsabs.harvard.edu/abs/2020ApJ...893L..29B> (visited on 02/22/2024).
 - [5] George Howard Darwin and James Whitbread Lee Glaisher. “I. On the bodily tides of viscous and semi-elastic spheroids, and on the ocean tides upon a yielding nucleus”. In: *Philosophical Transactions of the Royal Society of London* 170 (Jan. 1997). Publisher: Royal Society, pp. 1–35. DOI: 10.1098/rstl.1879.0061. URL: <https://royalsocietypublishing.org/doi/10.1098/rstl.1879.0061> (visited on 02/24/2024).
 - [6] *Exoplanet Transit Database*. URL: <http://var2.astro.cz/ETD/index.php> (visited on 03/21/2024).
 - [7] P. Goldreich. “On the eccentricity of satellite orbits in the solar system”. In: *Monthly Notices of the Royal Astronomical Society* 126 (Jan. 1, 1963). ADS Bibcode: 1963MNRAS.126..257G, p. 257. ISSN: 0035-8711. DOI: 10.1093/mnras/126.3.257. URL: <https://ui.adsabs.harvard.edu/abs/1963MNRAS.126..257G> (visited on 02/24/2024).
 - [8] Peter Goldreich and Steven Soter. “Q in the Solar System”. In: *Icarus* 5 (Jan. 1, 1966). ADS Bibcode: 1966Icar....5..375G, pp. 375–389. ISSN: 0019-1035. DOI: 10.1016/0019-1035(66)90051-0. URL: <https://ui.adsabs.harvard.edu/abs/1966Icar....5..375G> (visited on 02/24/2024).
 - [9] Richard Greenberg. “Frequency Dependence of Tidal q”. In: *The Astrophysical Journal* 698 (June 1, 2009). ADS Bibcode: 2009ApJ...698L..42G, pp. L42–L45. ISSN: 0004-637X. DOI: 10.1088/0004-637X/698/1/L42. URL: <https://ui.adsabs.harvard.edu/abs/2009ApJ...698L..42G> (visited on 03/05/2024).
 - [10] Simone R. Hagey, Billy Edwards, and Aaron C. Boley. “Evidence of Long-Term Period Variations in the Exoplanet Transit Database (ETD)”. In: *The Astronomical Journal* 164.5 (Nov. 1, 2022), p. 220. ISSN: 0004-6256, 1538-3881. DOI: 10.3847/1538-3881/ac959a. arXiv: 2209.10752[astro-ph]. URL: <http://arxiv.org/abs/2209.10752> (visited on 02/23/2024).
 - [11] Brad Hansen. “Calibration of Equilibrium Tide Theory for Extrasolar Planet Systems”. In: *The Astrophysical Journal* 723.1 (Nov. 1, 2010), pp. 285–299. ISSN: 0004-637X, 1538-4357. DOI: 10.1088/0004-637X/723/1/285. arXiv: 1009.3027[astro-ph]. URL: <http://arxiv.org/abs/1009.3027> (visited on 03/05/2024).
 - [12] Benjamin J. Hord et al. “The Discovery of a Planetary Companion Interior to Hot Jupiter WASP-132 b”. In: *The Astronomical Journal* 164.1 (July 1, 2022), p. 13. ISSN: 0004-6256, 1538-3881. DOI: 10.3847/1538-3881/ac6f57. arXiv: 2205.02501[astro-ph]. URL: <http://arxiv.org/abs/2205.02501> (visited on 02/22/2024).

- [13] Nawal Husnool et al. “Observational constraints on tidal effects using orbital eccentricities*”. In: *Monthly Notices of the Royal Astronomical Society* 422.4 (June 1, 2012), pp. 3151–3177. ISSN: 0035-8711. DOI: 10.1111/j.1365-2966.2012.20839.x. URL: <https://doi.org/10.1111/j.1365-2966.2012.20839.x> (visited on 03/05/2024).
- [14] Ekaterina S. Ivshina and Joshua N. Winn. “TESS Transit Timing of Hundreds of Hot Jupiters”. In: *The Astrophysical Journal Supplement Series* 259 (Apr. 1, 2022). ADS Bibcode: 2022ApJS..259...62I, p. 62. ISSN: 0067-0049. DOI: 10.3847/1538-4365/ac545b. URL: <https://ui.adsabs.harvard.edu/abs/2022ApJS..259...62I> (visited on 03/01/2024).
- [15] Brian Jackson, Rory Barnes, and Richard Greenberg. “Observational Evidence for Tidal Destruction of Exoplanets”. In: *The Astrophysical Journal* 698 (June 1, 2009). ADS Bibcode: 2009ApJ...698.1357J, pp. 1357–1366. ISSN: 0004-637X. DOI: 10.1088/0004-637X/698/2/1357. URL: <https://ui.adsabs.harvard.edu/abs/2009ApJ...698.1357J> (visited on 02/27/2024).
- [16] Brian Jackson, Richard Greenberg, and Rory Barnes. “Tidal Evolution of Close-in Extra-Solar Planets”. In: *The Astrophysical Journal* 678.2 (May 10, 2008), pp. 1396–1406. ISSN: 0004-637X, 1538-4357. DOI: 10.1086/529187. arXiv: 0802.1543[astro-ph]. URL: <http://arxiv.org/abs/0802.1543> (visited on 02/27/2024).
- [17] Yair Judkovsky, Aviv Ofir, and Oded Aharonson. *The Advantages of Global Photometric Models in Fitting Transit Variations*. Nov. 12, 2023. DOI: 10.48550/arXiv.2311.06948. arXiv: 2311.06948[astro-ph]. URL: <http://arxiv.org/abs/2311.06948> (visited on 03/01/2024).
- [18] Boris A. Kagan and Jürgen Sündermann. “Dissipation of Tidal Energy, Paleotides, and Evolution of the Earth–Moon System”. In: *Advances in Geophysics*. Ed. by Renata Dmowska and Barry Saltzman. Vol. 38. Elsevier, Jan. 1, 1996, pp. 179–266. DOI: 10.1016/S0065-2687(08)60021-7. URL: <https://www.sciencedirect.com/science/article/pii/S0065268708600217> (visited on 02/24/2024).
- [19] Laurel Kaye et al. “Transit timings variations in the three-planet system: TOI-270”. In: *Monthly Notices of the Royal Astronomical Society* 510 (Mar. 1, 2022). ADS Bibcode: 2022MNRAS.510.5464K, pp. 5464–5485. ISSN: 0035-8711. DOI: 10.1093/mnras/stab3483. URL: <https://ui.adsabs.harvard.edu/abs/2022MNRAS.510.5464K> (visited on 03/01/2024).
- [20] A. Kokori et al. “ExoClock Project III: 450 new exoplanet ephemerides from ground and space observations”. In: *The Astrophysical Journal Supplement Series* 265.1 (Mar. 1, 2023), p. 4. ISSN: 0067-0049, 1538-4365. DOI: 10.3847/1538-4365/ac9da4. arXiv: 2209.09673[astro-ph]. URL: <http://arxiv.org/abs/2209.09673> (visited on 02/23/2024).
- [21] G. Kovács, S. Zucker, and T. Mazeh. “A box-fitting algorithm in the search for periodic transits”. In: *Astronomy and Astrophysics* 391 (Aug. 1, 2002). ADS Bibcode: 2002A&A...391..369K, pp. 369–377. ISSN: 0004-6361. DOI: 10.1051/0004-6361:20020802. URL: <https://ui.adsabs.harvard.edu/abs/2002A&A...391..369K> (visited on 02/29/2024).

- [22] Laura Kreidberg. “batman: BASic Transit Model cAlculationN in Python”. In: *Publications of the Astronomical Society of the Pacific* 127.957 (Nov. 2015), pp. 1161–1165. ISSN: 00046280, 15383873. DOI: 10.1086/683602. arXiv: 1507.08285[astro-ph]. URL: <http://arxiv.org/abs/1507.08285> (visited on 02/29/2024).
- [23] Michel Mayor and Didier Queloz. “A Jupiter-mass companion to a solar-type star”. In: *Nature* 378 (Nov. 1, 1995). ADS Bibcode: 1995Natur.378..355M, pp. 355–359. ISSN: 0028-0836. DOI: 10.1038/378355a0. URL: <https://ui.adsabs.harvard.edu/abs/1995Natur.378..355M> (visited on 02/22/2024).
- [24] Carl D. Murray and Stanley F. Dermott. *Solar System Dynamics*. 1st ed. Cambridge University Press, Feb. 13, 2000. ISBN: 978-0-521-57295-8 978-0-521-57597-3 978-1-139-17481-7. DOI: 10.1017/CB09781139174817. URL: <https://www.cambridge.org/core/product/identifier/9781139174817/type/book> (visited on 02/24/2024).
- [25] NASA - *Eclipse Predictions and Earth’s Rotation*. URL: <https://eclipse.gsfc.nasa.gov/SEhelp/rotation.html> (visited on 02/24/2024).
- [26] NASA *Exoplanet Archive*. URL: <https://exoplanetarchive.ipac.caltech.edu/> (visited on 03/05/2024).
- [27] Gordon I. Ogilvie. “Tidal dissipation in stars and giant planets”. In: *Annual Review of Astronomy and Astrophysics* 52.1 (Aug. 18, 2014), pp. 171–210. ISSN: 0066-4146, 1545-4282. DOI: 10.1146/annurev-astro-081913-035941. arXiv: 1406.2207[astro-ph]. URL: <http://arxiv.org/abs/1406.2207> (visited on 03/02/2024).
- [28] Kishore C. Patra et al. “The Continuing Search for Evidence of Tidal Orbital Decay of Hot Jupiters”. In: *The Astronomical Journal* 159 (Apr. 1, 2020). ADS Bibcode: 2020AJ....159..150P, p. 150. ISSN: 0004-6256. DOI: 10.3847/1538-3881/ab7374. URL: <https://ui.adsabs.harvard.edu/abs/2020AJ....159..150P> (visited on 03/01/2024).
- [29] Michael Perryman. *The Exoplanet Handbook*. 2nd ed. Cambridge: Cambridge University Press, 2018. ISBN: 978-1-108-41977-2. DOI: 10.1017/9781108304160. (Visited on 03/05/2024).
- [30] Frédéric Pont. “Empirical evidence for tidal evolution in transiting planetary systems”. In: *Monthly Notices of the Royal Astronomical Society* 396.3 (July 1, 2009), pp. 1789–1796. ISSN: 0035-8711. DOI: 10.1111/j.1365-2966.2009.14868.x. URL: <https://doi.org/10.1111/j.1365-2966.2009.14868.x> (visited on 03/05/2024).
- [31] Robert J. Siverd et al. “KELT-1b: A Strongly Irradiated, Highly Inflated, Short Period, 27 Jupiter-mass Companion Transiting a mid-F Star”. In: *The Astrophysical Journal* 761.2 (Dec. 20, 2012), p. 123. ISSN: 0004-637X, 1538-4357. DOI: 10.1088/0004-637X/761/2/123. arXiv: 1206.1635[astro-ph]. URL: <http://arxiv.org/abs/1206.1635> (visited on 03/05/2024).
- [32] *TESS observations*. URL: <https://tess.mit.edu/science/observations/> (visited on 03/06/2024).

- [33] Jake D. Turner, Andrew Ridden-Harper, and Ray Jayawardhana. “Decaying Orbit of the Hot Jupiter WASP-12b: Confirmation with TESS Observations”. In: *The Astronomical Journal* 161.2 (Feb. 1, 2021), p. 72. ISSN: 0004-6256, 1538-3881. DOI: 10.3847/1538-3881/abd178. arXiv: 2012.02211[astro-ph]. URL: <http://arxiv.org/abs/2012.02211> (visited on 03/01/2024).
- [34] C. A. Watson and T. R. Marsh. “Orbital period variations of hot-Jupiters caused by the Applegate effect”. In: *Monthly Notices of the Royal Astronomical Society* (Apr. 2010), no–no. ISSN: 00358711, 13652966. DOI: 10.1111/j.1365-2966.2010.16602.x. arXiv: 1003.0340[astro-ph]. URL: <http://arxiv.org/abs/1003.0340> (visited on 03/01/2024).
- [35] A. Wolszczan and D. A. Frail. “A planetary system around the millisecond pulsar PSR1257 + 12”. In: *Nature* 355.6356 (Jan. 1992). Number: 6356 Publisher: Nature Publishing Group, pp. 145–147. ISSN: 1476-4687. DOI: 10.1038/355145a0. URL: <https://www.nature.com/articles/355145a0> (visited on 02/22/2024).